J|A|C|S
COMMUNICATIONS

Published on Web 06/01/2006

Germanium Telluride Nanowires and Nanohelices with Memory-Switching Behavior

Dong Yu, Junqiao Wu, Qian Gu, and Hongkun Park*

Department of Chemistry and Chemical Biology, Harvard University, 12 Oxford Street, Cambridge, Massachusetts 02138

Received April 11, 2006; E-mail: hongkun_park@harvard.edu

Chalcogenides undergoing crystalline−amorphous (order−disorder) phase transitions exhibit distinct resistance states that can be reversibly switched by temperature or electric field.[1−4] These "phase-change" compounds are the material bases for nonvolatile optical memory, such as CD and DVD,[3] and they are now being actively investigated as a medium for universal solid-state memory that may replace dynamic and flash random access memories.[4] Despite their widespread use, however, the exact mechanism of their respective phase changes is still under debate.[2,5] Moreover, the evolution of the phase-change properties as a function of material size has not been fully explored.

Over the past decades, the chemical methods to prepare various nanostructures have advanced considerably. Although early synthesis efforts were directed mostly toward nanocrystal quantum dots[6−8] and IV, III−V semiconductor nanowires (NWs),[9,10] new methods to prepare metal oxide[11−17] and chalcogenide[18,19] NWs have also begun to emerge. The preparation and characterization of nanoscale phase-change materials should provide valuable information on the size scaling of the phase-switching properties and may also provide insight into the mechanism that cannot be gleaned from experiments on bulk materials.

Here we report the synthesis of single-crystalline germanium telluride (GeTe) NWs and nanohelices (NHs) with reproducible phase-switching properties. Bulk GeTe has long served as a prototype for phase-change materials as a result of its simple composition and structure.[20−22] Crystalline (amorphous) GeTe is a semiconductor with a band gap of ∼0.1 (0.8) eV, with a room-temperature resistivity of $\sim 10^{-4}$ (10^{3}) Ω·cm.[22] Amorphous GeTe can be obtained by cooling molten GeTe rapidly ($\sim 10^{11}$ K s^{-1})[3] and can be converted back to the crystalline phase by heating it above the glass transition temperature $T_g \approx 145$ °C.

The synthesis of GeTe NWs and NHs was achieved by a vapor transport method, assisted by metal nanoparticle catalysts.[10,23] Bulk GeTe (99.99%, Sigma-Aldrich) was evaporated at the center of a horizontal tube furnace, and the reaction product was collected downstream on a SiO_2 substrate covered with colloidal Au nanoparticles (∼5−10 nm in diameters). Optimum source temperature (T), pressure (P), time (t), and Ar carrier gas flow rate (k_{flow}) for the growth of NWs and NHs were $T = 400$ °C, $P = 10$ Torr, $t = 8$ h, and $k_{flow} = 140$ sccm. The reactions at lower temperatures ($T = \sim 200-300$ °C) yielded Te NWs, whereas high-temperature reactions ($T > 500$ °C) yielded thicker GeTe NWs mixed with crystalline chunks. The NWs and NHs composed of GeTe were obtained only in the presence of Au nanoparticles.

Figure 1a shows a representative scanning electron microscopy (SEM) image of as-grown products and confirms that the reaction produces predominantly NWs and NHs. Energy-dispersive X-ray spectrometry (EDS) analyses show that Ge and Te are present in a 1:1 ratio in these structures (Figure S1 in Supporting Information). Images of the reaction products from multiple reaction runs show

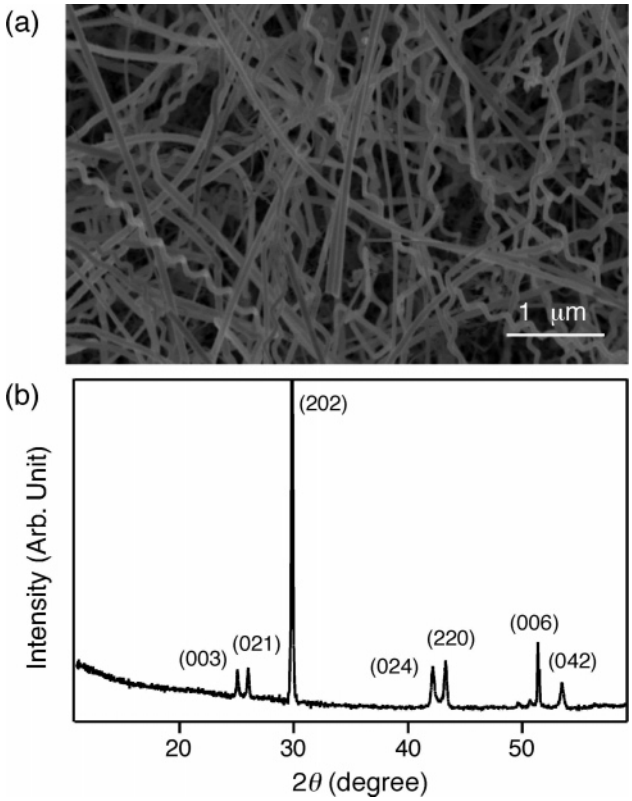

Figure 1. (a) SEM image of GeTe NWs and NHs, as grown on a SiO_2 substrate and (b) XRD pattern of the reaction product.

that the average diameter of GeTe NWs is 65 ± 20 nm with lengths reaching up to 50 μm. Typical GeTe NHs have an average helix diameter of 135 ± 30 nm, with widely varying pitch (Figures S2 and S3 in Supporting Information).

The structures of the GeTe NWs and NHs were examined using X-ray diffraction (XRD) and transmission electron microscopy (TEM). Figure 1b shows a representative XRD pattern of an as-synthesized sample and demonstrates unambiguously that NWs and NHs exhibit the low-temperature, rhombohedral form of GeTe (JCPDS file 47-1079). The TEM images shown in Figure 2 also confirm the single-crystallinity of NWs and NHs. Selected area electron diffraction (SAED) patterns from individual NWs and NHs indicate that a majority of NWs grow along the [220] direction (∼20% of NWs also grow along the [003] and [202] direction), while the helical axes of NHs always coincide with the [202] direction. The SAED patterns did not change when the electron-beam spot was moved along NW and NH lengths, indicating that they are single crystals.

The fact that the Au nanoparticles are necessary for the synthesis suggests that GeTe NWs and NHs are produced via metal-catalyzed

10.1021/ja0625071 CCC: $33.50

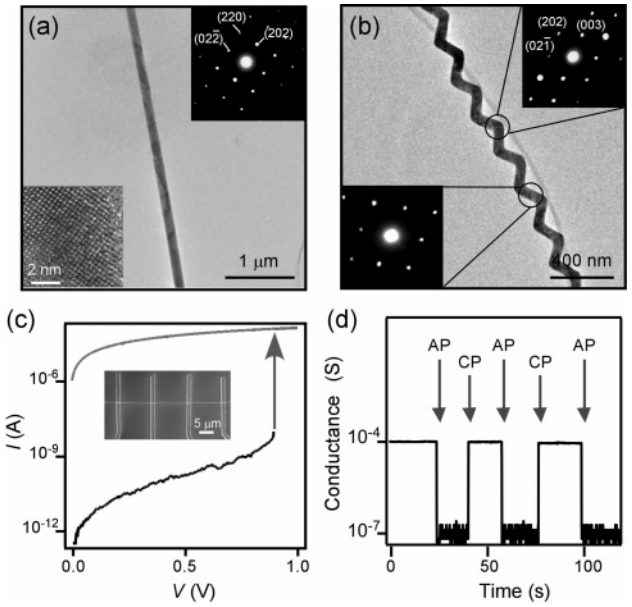

Figure 2. (a) TEM image of a GeTe NW. Upper inset: SAED pattern indexed for rhombohedral GeTe. Lower inset: High-resolution TEM image. (b) TEM image of a GeTe NH. Insets: SAED patterns obtained at two different locations. (c) $I-V$ characteristics of a crystalline (upper gray)/amorphous (lower black) GeTe NW device. Amorphous NWs spontaneously convert to a crystalline form when V exceeds V_{th}. (d) Conductance of a NW device upon application of amorphization (AP) and crystallization (CP) voltage pulses. In AP, $V = 4$ V and $\tau_{am} = 500$ ns, while in CP, $V = 1$ V and $\tau_{cryst} = 10$ ms.

vapor−liquid−solid growth.[10,23] Indeed, the TEM investigations indicate that some NWs and NHs have GeTe/Au alloy nanoparticles attached at the ends, providing evidence for this mechanism (Figure S4 in Supporting Information). The growth of NHs with variable pitch is difficult to understand based simply on the structure of the underlying GeTe lattice. One possible explanation may be the different growth speeds for opposite NH surfaces at the metal−GeTe interfaces,[24] but the exact mechanism needs further elucidation.

The phase-change characteristics of individual GeTe NWs were investigated by measuring the current (I) − voltage (V) characteristics of a NW device. The devices were fabricated by transferring NWs to a SiO_2-covered Si substrate either mechanically or via drop casting after sonication in isopropyl alcohol. Nickel contacts were then defined by standard electron-beam lithography. The completed devices were covered with ∼40-nm thick SiO_2 to prevent oxidation and evaporation of GeTe. The inset to Figure 2c shows a SEM image of a typical device.

The typical resistivity of the single-crystalline GeTe NWs was $\sim 10^{-4}$ Ω·cm at room temperature, and it increased with increasing temperature, consistent with the metallic behavior of bulk GeTe.[22] These metallic GeTe NWs could be amorphized by melting and cooling them rapidly via a short voltage pulse, as shown in Figure 2c,d.[4] Specifically, when the voltage pulse with a magnitude of 4 V and temporal width τ_{am} of ∼100−500 ns was applied, the resistance suddenly increased by a factor of $\sim 10^3-10^7$, signaling the occurrence of a crystalline-to-amorphous transition. After switching, the device remained in the high resistance state as long as V was kept below 0.5 V. Importantly, four-probe measurements of the same devices showed that this resistance increase originated from the NWs themselves and not from the metal−NW contacts. The magnitude of the resistance jump increased with τ_{am}, suggesting that the size of the amorphous domain depends on the Joule heating power applied to the device.

The reverse, amorphous-to-crystalline transition could be induced reproducibly either by thermal annealing above T_g under inert gas or by voltage-induced Joule heating.[4] The voltage-induced change is particularly important as it is a prerequisite for realizing purely electrical nonvolatile memory devices. As shown in Figure 2c, when V above a threshold (V_{th}: typically ranging from 0.5 to 2 V) was applied to the amorphous NW device for τ_{cryst} exceeding 1 ms, the resistance of the device dropped sharply by up to 7 orders of magnitude. After switching, the device remained highly conductive, even when the voltage was reduced to zero. The amorphization−crystallization cycle could be repeated multiple times in the same device, as clearly demonstrated in Figure 2d. In the recrystallization step, low V and long τ_{cryst} allowed the slow heating and cooling of GeTe and thus ensured that NWs have time to recrystallize properly.[22] It was also found that the values of V_{th} and τ_{cryst} generally increased with τ_{am}, corroborating the correlation between the amorphous domain size and the τ_{am}.

Single-crystalline GeTe NWs and NHs reported here may provide a convenient and promising material for future nonvolatile memory technology. Moreover, the reversible, nonvolatile resistance switching of GeTe NWs should allow the fundamental investigation of the size scaling of the phase-change characteristics as well as the detailed study of the phase-change mechanism.

Acknowledgment. This work is supported by the NSF Career award, Harvard NSEC award, and Samsung Electronics. We thank L. Ouyang, S. Weinman, D. Bell, Y. Lu, and W. Croft for scientific discussions and technical assistance.

Supporting Information Available: EDS data of GeTe NW and NH samples; histograms of NW diameters; SEM and TEM images of NHs; TEM image and EDS data of a NW with a catalyst particle at the end. This material is available free of charge via the Internet at http://pubs.acs.org.

References

(1) Ovshinsky, S. R. *Phys. Rev. Lett.* **1968**, *21*, 1450−1453.
(2) Adler, D.; Henisch, H. K.; Mott, N. *Rev. Mod. Phys.* **1978**, *50*, 209−220.
(3) Yamada, N.; Ohno, E.; Nishiuchi, K.; Akahira, N. *J. Appl. Phys.* **1991**, *69*, 2849−2856.
(4) Lankhorst, M. H. R.; Ketelaars, B. W. S. M. M.; Wolters, R. A. M. *Nat. Mater.* **2005**, *4*, 347−352.
(5) Greer, A. L.; Mathur, N. *Nature* **2005**, *437*, 1246−1247.
(6) Alivisatos, A. P. *Science* **1996**, *271*, 933−937.
(7) Murray, C. B.; Kagan, C. R.; Bawendi, M. G. *Annu. Rev. Mater. Sci.* **2000**, *30*, 545−610.
(8) Peng, X.; Manna, L.; Yang, W.; Wickham, J.; Sher, E.; Kadavanich, A.; Alivisatos, A. P. *Nature* **2000**, *404*, 59−61.
(9) Cui, Y.; Wei, Q. Q.; Park, H. K.; Lieber, C. M. *Science* **2001**, *293*, 1289−1292.
(10) Hu, J.; Odom, T. W.; Lieber, C. M. *Acc. Chem. Res.* **1999**, *32*, 435−445.
(11) Huang, M. H.; Wu, Y.; Feick, H.; Tran, N.; Weber, E.; Yang, P. *Adv. Mater.* **2001**, *13*, 113−116.
(12) Yang, R.; Ding, Y.; Wang, Z. L. *Nano Lett.* **2004**, *4*, 1309−1312.
(13) Kong, X. Y.; Ding, Y.; Yang, R.; Wang, Z. L. *Science* **2004**, *303*, 1348−1351.
(14) Urban, J. J.; Yun, W. S.; Gu, Q.; Park, H. *J. Am. Chem. Soc.* **2002**, *124*, 1186−1187.
(15) Urban, J. J.; Ouyang, L.; Jo, M.-H.; Wang, D. S.; Park, H. *Nano Lett.* **2004**, *4*, 1547−1550.
(16) Guiton, B. S.; Gu, Q.; Prieto, A. L.; Gudiksen, M. S.; Park, H. *J. Am. Chem. Soc.* **2005**, *127*, 498−499.
(17) Patzke, G. R.; Krumeich, F.; Nesper, R. *Angew. Chem., Int. Ed.* **2002**, *41*, 2446−2461.
(18) Cho, K. S.; Talapin, D. V.; Gaschler, W.; Murray, C. B. *J. Am. Chem. Soc.* **2005**, *127*, 7140−7147.
(19) Hor, Y. S.; Welp, U.; Xiao, Z. L.; Patel, U.; Mitchell, J. F.; Kwok, W. K.; Crabtree, G. W. *Appl. Phys. Lett.* **2005**, *87*, 142506.
(20) Chopra, K. L.; Bahl, S. K. *J. Appl. Phys.* **1969**, *40*, 4171−4178.
(21) Bahl, S. K.; Chopra, K. L. *J. Appl. Phys.* **1969**, *40*, 4940−4947.
(22) Bahl, S. K.; Chopra, K. L. *J. Appl. Phys.* **1970**, *41*, 2196−2212.
(23) Wu, Y. Y.; Yang, P. D. *J. Am. Chem. Soc.* **2001**, *123*, 3165−3166.
(24) Amelinckx, S.; Zhang, X. B.; Bernaerts, D.; Zhang, X. F.; Ivanov, V.; Nagy, J. B. *Science* **1994**, *265*, 635−639.

JA0625071